Available online at www.sciencedirect.com
ScienceDirect
Journal of the European Ceramic Society 29 (2009) 363–367
www.elsevier.com/locate/jeurceramsoc

Unidirectional all-oxide mini-composites with crack-deflecting $NdPO_4$ interface

C. Kaya [a,*], E.G. Butler [b]

[a] *Yildiz Technical University, Faculty of Chemistry and Metallurgy, Department of Metallurgical and Materials Engineering, Davutpasa Campus, Esenler, Istanbul, Turkey*
[b] *The University of Birmingham, IRC in Materials Processing and School of Metallurgy and Materials, Edgbaston, Birmingham B15 2TT, UK*

Received 6 February 2008; received in revised form 20 May 2008; accepted 6 June 2008
Available online 21 July 2008

Abstract

Unidirectional Nextel 720™ fibers were coated with crack-deflecting $NdPO_4$ interface using dip coating and infiltrated with silica-free alumina matrix using electrophoretic deposition followed by drying and pressureless sintering at 1200 °C in an attempt to manufacture oxide-based model 'mini-composites' which are less complex to produce in a short time and which therefore allow rapid results for mechanical and microstructural characterisation. This material is targeted for use at 1200 °C in an oxidising atmosphere and has shown an excellent tensile strength value of 1.2 GPa and flexural strengths of 894 MPa at room temperature and 761 MPa at 1300 °C in unidirectional form.

Keywords: Composites; Al_2O_3; Interface; Mini-composites; $NdPO_4$

1. Introduction

High strength continuous fiber-reinforced ceramic composites (CMCs) have emerged as leading candidates in gas-turbine applications and power generation systems where future requirements for increased operating temperature, reduction in weight and in exhaust emissions are becoming difficult to meet using conventional metallic alloys.[1–6] The physical and mechanical properties of new generation oxide/oxide CMCs enable innovative solutions for problems with materials in thermal protection systems and liners in gas-turbine engines, rocket engine, hot gas filter technologies, fire prevention, catalytic converters, soot filters and medical applications.[7–9] As a consequence, many gas-turbine manufactures are now placing greater emphasis on the evaluation of oxide/oxide components with enhanced high temperature stability and long service life in oxidising environments.[10–20] Although the reinforcement fibers and matrices are brittle, the obtained composites display quasi-ductile deformation behaviour due to operation of crack deflection, fiber–matrix debonding, crack bridging and fiber pull-out mechanisms that all contribute to increasing toughness.[1–7,9–15,21] To obtain ideal damage-tolerant behaviour, two concepts have been developed so far[4,12,13,22]; the first one is to create a relatively weak bonding between fibers and the matrix by coating the fibers with suitable crack-deflecting interface materials, such as ZrO_2 or $NdPO_4$ that do not react with the ceramic matrices/fibers or fugitive carbon that creates a gap at the fiber/matrix interface; the second one is to use highly porous matrices to isolate fibers from matrix cracks so that quasi-ductile deformation can be obtained as the cracks do not have a continuous front since the matrix is held together by grain pairs but the overall strength is quite low in this case due to the presence of high porosity content up to 50%.

In the present work, alumina ceramic matrix is reinforced with $NdPO_4$-coated unidirectional ceramic fibers in an attempt to manufacture small damage-tolerant model composite samples called 'mini-composites' suitable for mechanical testing and microstructural observations in a short processing time.

2. Experimental work

2.1. Materials

Sinter-active high purity alumina powders (Tai-Micron, Japan) with an average particle size of 160 nm and surface area

* Corresponding author. Tel.: +90 2123834713; fax: +90 2123834665.
E-mail address: cngzky@yahoo.co.uk (C. Kaya).

0955-2219/$ – see front matter © 2008 Elsevier Ltd. All rights reserved.
doi:10.1016/j.jeurceramsoc.2008.06.009

of 14.3 m^2/g were used as the matrix materials. Alumina powders were first dispersed in distilled water with the additions of dispersant, liquid binder which is a water-based acrylic polymer (Duramax B1014, Chesham Chemicals Ltd., UK) and a mixture of boehmite (γ-AlOOH) and colloidal Y_2O_3 as sintering aids with average particle sizes of 20 and 10 nm, respectively and magnetically stirred for 2 h followed by mechanical ball-milling with alumina balls for 8 h and finally ultrasonication for 0.5 h. The amount of sintering aids was 2 wt.% of the total powder and the solid-loading of the final suspension was 85 wt.% and the pH was adjusted to be around 4 (the weight ratio of boehmite to Y_2O_3 was 1:1).

Unidirectional fiber bundles extracted from eight-harness satin woven mullite fiber mats (Nextel™ 720, 1500-denier yarn, 3M, USA) were used as reinforcement materials. Each fiber bundle contains approximately 1500 filaments with an average diameter of 12 μm. Before the extraction process, the woven fiber mats were pre-treated by desizing at 500 °C for 1 h to remove the organic protection layer from the fiber surface and then the bundles were extracted from the desized mats.

$NdPO_4$ interface material was prepared by the neutral reaction of neodymium nitrate with ammonium di-hydrogen phosphate (ADPH) at room temperature. Equimolar amounts of $Nd(NO_3)_3$ and ADPH were dissolved into water to make 0.25 M solutions. Mixing of the two solutions by vigorous stirring and heating was followed by filtration. The resultant gel filtrate was then dried and calcined at 1000 °C for 3 h to yield stoichiometric $NdPO_4$ monazite powder with an average particle size of 60 nm. A 15-wt.% aqueous-based suspension was prepared by ball milling for 4 h with the pH value adjusted to be 3.

2.2. Fiber coating

The required number of bundles was extracted from the mat and then immersed in an ammonia-based solution, consisting of an ammonium salt of polymethacrylic acid (Versical KA21, pH: 9, Allied colloids, UK) in order to create a strong negative surface charge on the fiber surface. Surface-modified fiber bundle was then dipped in $NdPO_4$ suspension for 1 min to allow $NdPO_4$ particles to fully cover the fibers. Coated fiber bundles were then sintered at 600 °C for 0.5 h to increase the adhesion between the fiber and the coating layer.

2.3. Processing of mini-composites

Dip-coated fiber bundle is impregnated with nano-size alumina ceramic particles by electrophoretic deposition (EPD) using a deposition voltage of 10 V for 3 min. The details of the technique can be found elsewhere.[17–19,23–27] Coated and electrophoretically deposited fiber bundles were then put in a polymer-based tube with an inner diameter of 4 mm as shown in Fig. 1. Then a hot gun was used to heat the surface of the plastic tube up to 150 °C so that it shrinks and squeezes the bundles homogeneously. The specimens compacted within the plastic tube were then removed by cutting the plastic tube and pressureless sintered at 1200 °C for 2 h. The sintered mini-composites

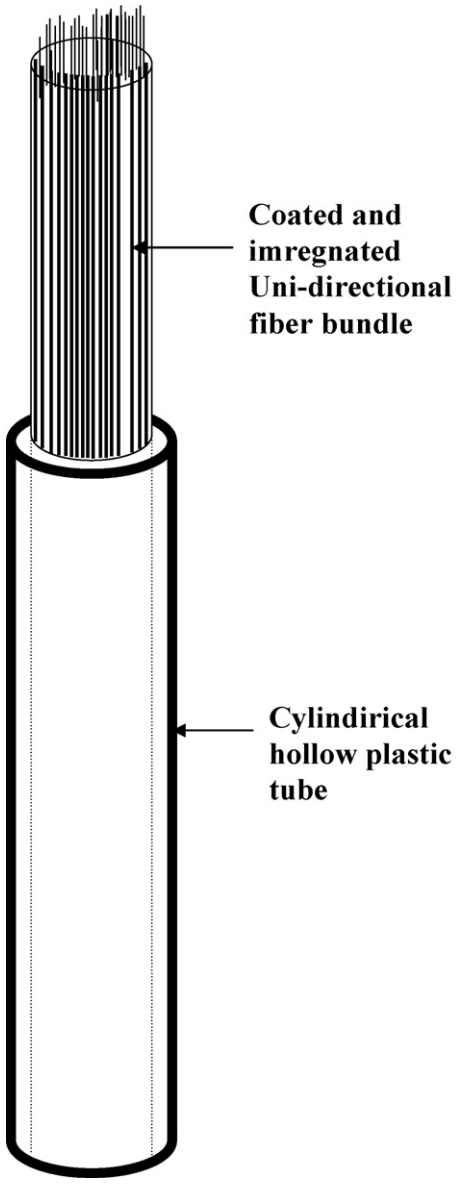

Fig. 1. Schematic representation of the model mini-composites produced.

with a diameter of 2 mm and 40 vol.% fiber loading were then cut for mechanical testing and microstructural observations.

2.4. Mechanical tests

Tubular tensile and flexural test specimens with a length of 10 cm were cut from the sintered composites. Tensile ends of the specimen were fixed in tubular aluminium tabs using a polymeric resin which was cured at 280 °C for 1 h in order to provide a strong adhesion between the sample and aluminium tabs so that sliding of the sample from grips was prevented during tensile tests. Room and high temperature four-point bend tests were performed on an Instron Testing machine fitted with a furnace which has tungsten mesh elements enabling tests to be carried out at temperatures up to 1500 °C. Specimens to be tested at 1300 °C, were held at the test temperature for at least 1 h prior the testing to allow the system to equilibrate and to ensure that

the specimen was at this temperature. Tensile tests were performed at room temperature. For flexural and tensile tests, a constant cross-head speed of 0.5 mm/min was used. For all the mechanical results reported, seven samples were used for each value by eliminating the highest and the lowest values and taking the average value of the remaining five readings.

2.5. Microstructural characterisation

Microstructural examinations were carried out on sintered and fractured composite samples using a high-resolution field emission gun (FEG) SEM (FX-4000, Jeol Ltd., Japan). Further detail observations were carried out using transmission electron microscopy (TEM, Jeol Ltd., Japan, 4000 FX TEM) operating at 400 kV, and equipped with an energy dispersive X-Ray analysis (EDX) unit. Porosity (%) and pore size were measured using a mercury porosimeter (Hg Por, Micromechanics Instrument Corp., USA) using a penetrometer weight of 62.79 g, head pressure of 4.45 psia and penetration volume of 6.188 mL. Archimedes technique was also used for density measurements.

3. Results and discussion

Fig. 2 shows the SEM microstructure of dip-coated unidirectional Nextel 720^{TM} fibers with $NdPO_4$ interface material after sintering at 600 °C for 0.5 h indicating that the coating layer is very homogeneous, dense and its thickness is less than 2 μm. When oxide/oxide composites are designed for high temperature applications, it is fundamental that a compatible weak interface between the reinforcement fiber and ceramic matrix should be provided in order to obtain a damage-tolerant behaviour due to mechanisms of crack deflection, debonding and fiber pull-out that all contribute to increasing the toughness. Dense interfaces are also desirable as they protect the fibers at high temperature against heat and oxygen diffusion which may cause grain growth and loss in mechanical properties. Furthermore, it is well established that significant reduction in mechanical properties is actually caused by the fiber damage during processing and therefore the dense coating structure shown in Fig. 2 helps to protect the fiber's surface from flaws during manufacturing steps, especially during impregnation and consolidation within the hollow plastic tube subjected to heat. Fig. 2 also shows that the $NdPO_4$ coating layer is non-porous and quite dense and there is no visible evidence of reaction taking place between the coating layer and the fiber. Further examinations were also conducted using transmission electron microscopy to confirm that there was no reaction zone at the interfaces between $NdPO_4$ and fiber as in the TEM micrograph shown in Fig. 3. As shown in Fig. 3, the interfacial zone between the fiber and the $NdPO_4$ interface is very clear and there is no strong bonding at this point that proves the absence of any chemical reaction between the interface material and the fibers. TEM EDX analysis on the interfacial zone also indicated that there was no reaction product at that region that explained the absence of any undesirable reactions (see also Fig. 5b showing the clear surface of the pulled out fibers that also proves the absence of any strong bonding between the fibers and the interface materials). This is very important to improve the flaw tolerance and work of fracture of the composite and also to obtain non-catastrophic mode of failure due to presence of an interface which is weak enough to deflect propagating cracks which will lead to substantial energy dissipation and improve fracture toughness. Fig. 3 also shows that the grain size of the $NdPO_4$ interface is about 250 nm which explains the dense coating microstructure (see Fig. 2) resulted from sinter-active starting particles of $NdPO_4$.

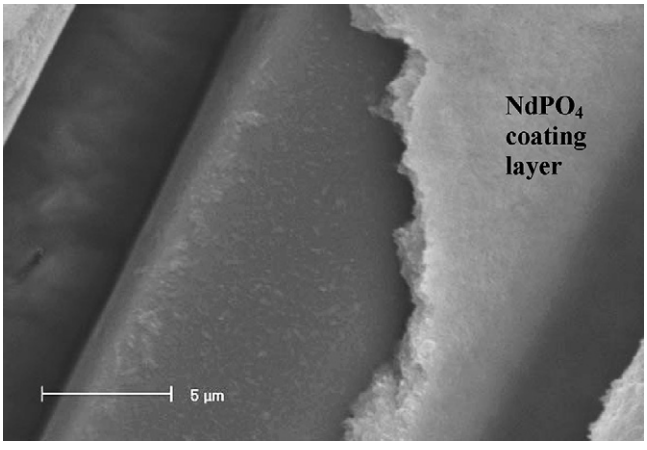

Fig. 2. SEM microstructure of dip-coated unidirectional Nextel 720^{TM} fiber with a crack-deflecting $NdPO_4$ interface after sintering at 600 °C for 0.5 h indicating the homogeneous and dense structure of the coating layer with a thickness of less than 2 μm.

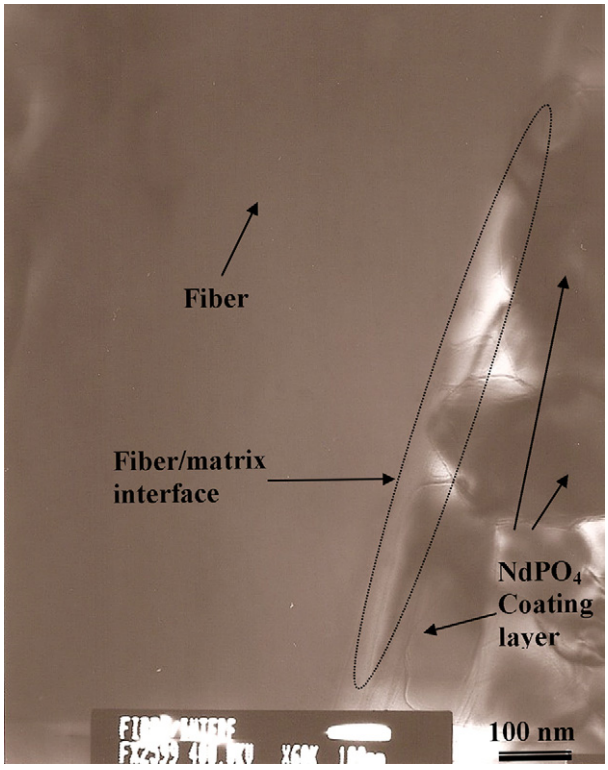

Fig. 3. Transmission electron microscopy (TEM) image of the composite sample containing $NdPO_4$ interface indicating that there is no reaction between the interface and the fiber.

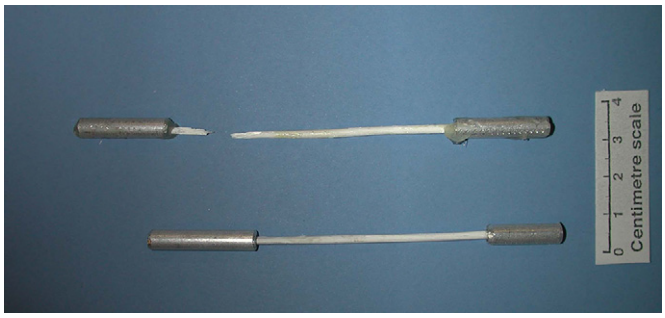

Fig. 4. An optical microscopy photo of the tensile test specimens of mini-composite containing unidirectional Nextel 720™ fiber reinforced alumina ceramic composite with $NdPO_4$ interface.

An optical microscopy image of the unidirectional fiber-reinforced mini-composites with $NdPO_4$ interface in tubular shape before and after tensile tests is shown in Fig. 4 indicating the size of the test sample (about 2 mm in diameter) and the arrangement of the tensile specimen using aluminium tabs. The final mini-composites tested contain a fiber volume fraction of 0.4, 16% porosity with an average pore size of 75 nm. The tensile strength of the mini-composite was determined to be 1203 MPa (1.2 GPa) with the presence of damage-tolerant behaviour. The tensile strength of the fiber bundle itself is 800 MPa.[28]

In order to analyse the fracture behaviour in detail, load–displacement curves of the mini-composites subjected to flexural tests at room temperature and 1300 °C are shown in Fig. 5a that indicates the behaviour of a typical fiber-reinforced composite behaviour with the absence of catastrophic failure. Flexural strengths of the mini-composites were determined to be 894 MPa at room temperature and 761 MPa at 1300 °C which indicated that only 15% reduction in flexural strength was seen at 1300 °C but no distinct change of damage-tolerant behaviour was seen at both test temperatures (see Fig. 5a). As shown in Fig. 5a, mini-composites display quasi-ductile deformation behaviour due to operation of crack deflection, fiber–matrix debonding, crack bridging and fiber pull-out mechanisms that are all operational at room temperature and 1300 °C. Up to the maximum load, the mini-composite sample showed linear-elastic deformation behaviour without any obvious damage until the first matrix cracks occurred (between stress levels of 40 and 100 MPa as expected), indicated by a step-wise decrease of load (as circled in Fig. 5a) at both temperatures. But at this load, sufficient load transfer from the matrix to the fibers was achieved and as a result the composite was still able to carry loads without catastrophic failure by the operation of fiber/matrix debonding and pull-out mechanisms. The weak nature of the $NdPO_4$ interface also allowed crack deflection to take place at the interface region that consumed significant part of the energy. Due to high strength and stiffness of the reinforcement fibers they are expected to fracture at very high level of stresses. As shown in Fig. 5a, there were sharp step-wise decreases in loads for the mini-composite samples subjected to flexural tests at both room temperature and 1300 °C that indicated the bundle type of failure. This type of fracture generally leads to a considerable fiber pull-out. This case was well proven by the SEM microstructure shown in Fig. 5b. Fracture surface of the mini-composite sample

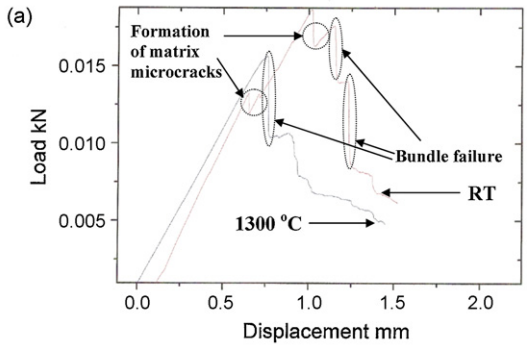

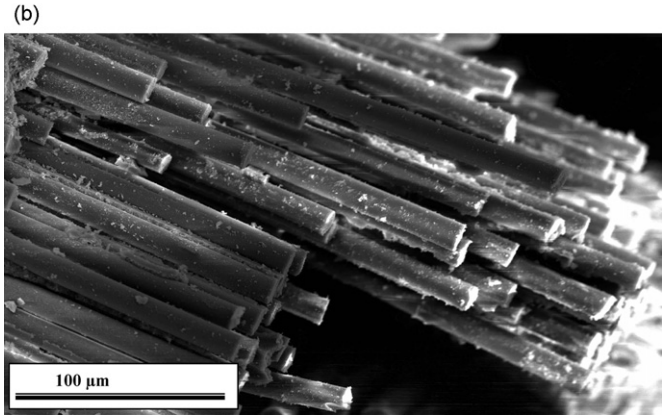

Fig. 5. (a) Load–displacement curves of four-point bend tested mini-composites (at room temperature and 1300 °C) with $NdPO_4$ interfaces and (b) fracture surface of tensile-tested mini-composite showing the presence of long fiber pull-out.

subjected to tensile test at room temperature is shown in Fig. 5b indicating the presence of long fiber pull-out and some degree of bundle fracture due to mechanisms, such as fiber/matrix debonding and crack deflection both initiated by the weak nature of the $NdPO_4$ interface. Fig. 5b also proves that crack-deflecting interface plays an important role in obtaining long fiber pull-out (pulled-out fiber lengths were observed to be longer than 300 μm under scanning electron microscope) which eventually leads to a pseudoplastic damage-tolerant behaviour. Combining the results presented in Figs. 2–5, it can be concluded that the mini-composites showed a very good room and high temperature flexural strength value with non-catastrophic failure behaviour due to possible two main reasons: (i) the presence of dense but crack-deflecting $NdPO_4$ coating layer that protects the fiber to be damaged during processing and against heat and (ii) low porosity content of 16% and small pore size. Therefore, the matrix properties (porosity level and pore size) and interface structure play a role and determine the overall damage-tolerant behaviour.

Overall, it is presented in the present work that reproducible model mini-CMCs are manufactured in a very short processing time using relatively simple and rapid processing techniques, namely dip coating and electrophoretic deposition to obtain quick mechanical and microstructural results that are both necessary for design and modelling purposes. Therefore time consuming several processing steps used for bulk composite processing (for example woven fiber-reinforced 2-D CMCs) to obtain mechanical test results can be eliminated. These

model mini-composites can be used to derive useful composite parameters including load transfer and fiber/matrix interfacial parameters that can all be used to design more complex composite systems.

4. Conclusions

Unidirectional Nextel 720™ fibers-reinforced alumina ceramic matrix mini-composites are fabricated using rapid and simple processing techniques of dip coating and electrophoretic deposition in order to obtain quick results from mechanical tests and microstructural observations. Pressureless sintered (1200 °C, 2 h) model mini-composites with an overall porosity content of 16%, fiber volume fraction of 0.4 and average pore size of less than 100 nm provide excellent room temperature tensile strength value of 1.2 GPa and flexural strengths of 894 MPa at room temperature and 761 MPa at 1300 °C. Quasi-ductile deformation (damage-tolerant) behaviour is achieved by dense but weak $NdPO_4$ interface that provides crack deflection, fiber–matrix debonding and fiber pull-out mechanisms (that all contribute to increasing toughness) to take place. All-oxide model mini-composites can be used to obtain quick mechanical and microstructural results that are both necessary for design and modelling purposes.

Acknowledgements

TUBITAK (Turkish Science and Technological Research Counsel) and Yıldız Technical University of Istanbul are acknowledged for financial support.

References

1. Chawla, K. K., Coffin, C. and Xu, Z. R., Interface engineering in oxide fibre/oxide matrix composites. *Int. Mater. Rev.*, 2000, **45**, 165–189.
2. Kaya, C., Butler, E. G., Selcuk, A., Boccaccini, A. R. and Lewis, M. H., Mullite (NextelTM 720) fibre-reinforced mullite matrix composites exhibiting favourable thermomechanical properties. *J. Eur. Ceram. Soc.*, 2002, **22**(13), 2333–2342.
3. Chawla, K. K., *Ceramic Matrix Composites*. Chapman & Hall, London, UK, 1998.
4. Lewis, M. H., Tye, E., Butler, E. G. and Doleman, P. A., Oxide CMCs: interphase synthesis and novel fibre development. *J. Eur. Ceram. Soc.*, 2000, **20**, 639644.
5. Warren, R. and Deng, S., Continuous fibre reinforced ceramic composites for very high temperatures. *Silic. Ind.*, 1996, **5**(6), 96–107.
6. Peters, P. W. M., Daniels, B., Clemens, F. and Vogel, W. D., Mechanical characterisation of mullite-based ceramic matrix composites at test temperatures up to 1200 °C. *J. Eur. Ceram. Soc.*, 2000, **20**, 531–535.
7. Holmquist, M. G., Radsick, T. C., Sudre, O. H. and Lange, F. F., Fabrication and testing of all-oxide CFCC tubes. *Composite Part A*, 2003, **34**, 163–170.
8. Razzel, A. G., Holquist, M., Molliex, L. and Sudre, O., Oxide/oxide ceramic matrix composites in gas turbine combusters. *ASME Paper 98-GT-30*. ASME, New York, 1998.
9. Beesley, C. P., The applications of CMCs in high integrity gas turbine engines. *Key Eng. Mater.*, 1997, **127–131**, 165–174.
10. Lewis, M. H., Tye, A., Butler, E. G. and Al-Dawery, I., Development of interfaces in oxide matrix composites. *Key. Eng. Mater.*, 1999, **164–165**, 351–356.
11. Zawada, L. P., Longitudinal and transthickness tensile behaviour of several oxide/oxide composites. *Ceram. Eng. Sci. Proc.*, 1998, **18**(3), 327–339.
12. Tu, W. C., Lange, F. F. and Evans, A. G., Concept for damage-tolerant ceramic composites with 'strong' interfaces. *J. Am. Ceram. Soc.*, 1996, **79**(2), 417–424.
13. Faber, K. T., Ceramic composite interfaces: Properties and design. *Annu. Rev. Mater. Sci.*, 1997, **27**, 499–524.
14. Kanka, B. and Schneider, H., Aluminosilicate fiber/mullite matrix composites with favorable high-temperature properties. *J. Eur. Ceram. Soc.*, 2000, **20**, 619–623.
15. Kaya, C., Gu, X., Al-Dawery, I. and Butler, E. G., Microstructural development of woven mullite fibre-reinforced mullite ceramic matrix composites by infiltration processing. *Sci. Technol. Adv. Mater.*, 2002, **3**(1), 35–44.
16. Kaya, C., He, J. Y., Gu, X. and Butler, E. G., Nanostructured ceramic powders by hydrothermal synthesis and their applications. *Micropor. Mesopor. Mater.*, 2002, **54**(1–2), 37–49.
17. Stoll, E., Mahr, P., Kruger, H. G., Kern, H., Thomas, B. J. C. and Boccaccini, A. R., Fabrication technologies for oxide-oxide ceramic matrix composites based on electrophoretic deposition. *J. Eur. Cerm. Soc.*, 2006, **26**(9), 1567–1576.
18. Stoll, E., Mahr, P., Kruger, H. G., Kern, H., Dlouhy and Boccaccini, A. R., Progress in the characterisation of structural oxide/oxide ceramic matrix composites fabricated by electrophoretic deposition (EPD). *Adv. Eng. Mater.*, 2006, **8**(4), 282–285.
19. Boccaccini, A. R., Kaya, C. and Krüger, H.-G., Application of the electrophoretic deposition technique in the fabrication of fibre reinforced ceramic and glass matrix composites. *Chem.-Ing.-Tech.*, 2001, **73**(5), 443–452.
20. Bansall, P. N., *Handbook of Ceramic Composites*. Kluwer Academic Publishers, Boston, USA, 2005.
21. Naslain, N., Lamon, J., Pailler, R., Bourrat, X., Guette, A. and Langlais, F., Micro/minicomposites: a useful approach to the design and development of non-oxide CMCs. *Composite Part A*, 1999, **30**, 537–547.
22. Lange, F. F., Tu, W. and Cevans, A. G., Processing of damage-tolerant, oxidation-resistant ceramic matrix composites by a precursor infiltration and pyrolysis method. *Mater. Sci. Eng. A*, 1995, **195**, 145–150.
23. Kaya, C., Kaya, F. and Boccaccini, A. R., Electrophoretic deposition infiltration of 2-D metal fibre-reinforced cordierite matrix composites of tubular shape. *J. Mater. Sci.*, 2002, **37**(19), 4145–4153.
24. Kaya, C., Kaya, F. and Boccaccini, A. R., Fabrication of stainless-steel-fiber-reinforced cordierite-matrix composites of tubular shape using electrophoretic deposition. *J. Am. Ceram. Soc.*, 2002, **85**(10), 2575–2577; Boccaccini, A. R., Kaya, C. and Chawla, K. K., Use of electrophoretic deposition in the processing of fibre reinforced ceramic and glass matrix composites: a review. *Composites Part A: Appl. Sci. Manuf.*, 2001, **32**(8), 997–1006.
25. Kaya, C., Kaya, F., Boccaccini, A. R. and Chawla, K. K., Fabrication and characterisation of Ni-coated carbon fibre-reinforced alumina ceramic matrix composites using electrophoretic deposition. *Acta Mater.*, 2001, **49**(7), 1189–1197.
26. Kaya, C., Boccaccini, A. R. and Chawla, K. K., Electrophoretic deposition forming of nickel-coated-carbon-fiber-reinforced borosilicate-glass–matrix composites. *J. Am. Ceram. Soc.*, 2000, **83**(8), 1885–1888.
27. Kaya, C., Boccaccini, A. R. and Trusty, P. A., Processing and characterisation of 2-D woven metal fibre-reinforced multilayer silica matrix composites using electrophoretic deposition and pressure filtration. *J. Eur. Ceram. Soc.*, 1999, **19**(16), 2859–2866.
28. Bansal, P. N., *Handbook of Ceramic Composites*. Kluwer Academic Publisher, Boston, 2005, pp. 3–33.